Supporting Information for

Aggregate-state-dependent photochromism and circularly polarized luminescence of a chiral biquinoline amphiphile

Chenyang Zhao,[‡a,b] Zujian Li,[‡a] Lukang Ji,[a] Hanxiao Wang,[a] Guanghui Ouyang*[a] and Minghua Liu[a,b]

[a.] *Beijing National Laboratory for Molecular Science (BNLMS) and CAS Key Laboratory of Colloid, Interface and Chemical Thermodynamics, Institute of Chemistry, Chinese Academy of Sciences, Beijing, 100190, China.*

[b.] *Green Catalysis Center and College of Chemistry, Zhengzhou University, Zhengzhou 450001, China.*

E-mail: ouyanggh@iccas.ac.cn

Contents

1. Synthesis and characterization

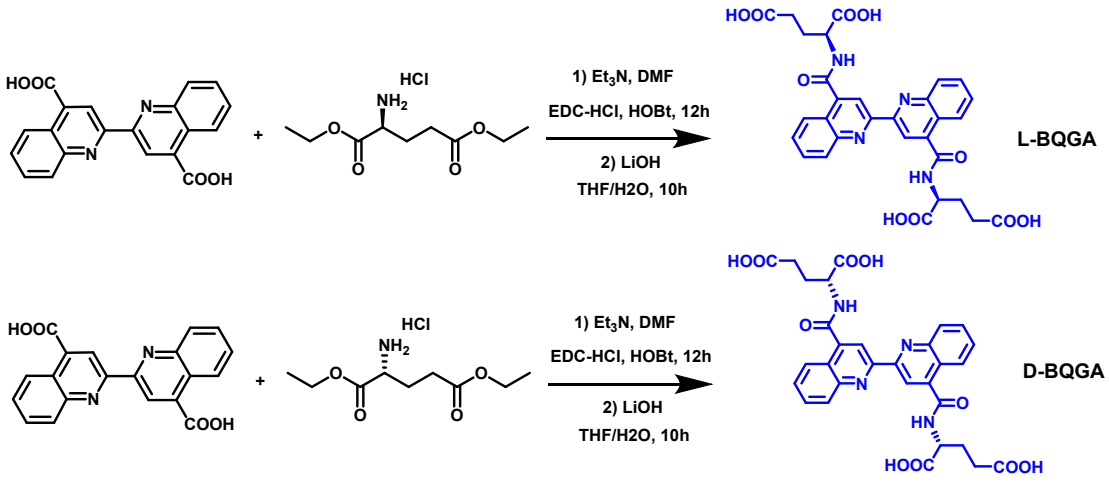

Scheme S1. Synthetic routes to ***L*-BQGA** and ***D*-BQGA**.

Synthesis of *L*-BQGA:

L-glutamic diethyl ester hydrochloride (1.46 g, 6.10 mmol) was dispersed in N, N'-dimethylformamide (100 mL) in a 250 mL round flask. Triethylamine (0.64 g, 6.38 mmol) was added and the mixture was stirred at RT for 1 h. Anhydrous 1-hydroxybenzotriazole (HOBt, 0.86 g, 6.20 mmol), 1-(3-dimethylaminopropyl) -3-ethylcarbodiimide hydrochloride (EDC•HCl, 1.22 g, 6.20 mmol) and 2,2'-biquinoline-4,4-dicarboxylic acid (1.00 g, 2.90 mmol) were added to the solution. The mixture was stirred at RT overnight. The reaction solution was detected by TLC (DCM/MeOH = 20 : 1). After the reaction was finished, the organic solvent was removed using rotary evaporator and dichloromethane was added to dissolve. the reaction mixture was washed with saturated $NaHCO_3$ aqueous solution for three times (3×200 mL) and washed with water for one time (200 mL). The organic phase was collected and dried over anhydrous Na_2SO_4. The obtained crude product was purified by column chromatography (silica gel, eluent: DCM/MeOH = 30 : 1) to give a white solid powder, *L*-BQGE. *L*-BQGE (0.90 g, 1.25 mmol) and lithium hydroxide (LiOH, 0.66 g, 15.70 mmol) were dispersed in 100 mL of mixed solvent (THF/H_2O = 1 : 1) in a 250 mL round flask. The mixture was stirred at RT overnight. The pH of the reaction solution was adjusted to 3 with hydrochloric acid. After evaporating part of

the tetrahydrofuran, yellow precipitates were formed. After filtration, the crude product was dissolved in 50 mL of hot methanol solution and 300 mL of water was then added to precipitate the product. The target product was obtained by filtration and drying. Yellow solid powder, 0.65 g, yield: 85.5 %.

^{1}H NMR (400 MHz, DMSO-d_6, 298 K), see **Figure S11:** δ = 13.50-11.69 (m, 2H), 9.23 (s, 2H), 8.81 (s, 2H), 8.28 (t, J = 7.4 Hz, 4H), 7.91 (t, J = 7.6 Hz, 2H), 7.75 (t, J = 7.8 Hz, 2H), 4.62-4.51 (m, 2H), 2.44 (d, J = 7.6 Hz, 4H), 2.14 (d, J = 7.7 Hz, 2H), 1.98 (m, 2H).

^{13}C NMR (100 MHz, DMSO-d_6, 298 K), see **Figure S12:**174.18, 173.50, 167.56, 154.79, 147.99, 144.07, 131.10, 130.23, 128.70, 126.08, 125.15, 116.63, 52.49, 30.84, 26.37.

HR-MALDI-TOF-MS, see **Figure S13:** m/z calcd. for $[M+H]^+$, $C_{30}H_{27}N_4O_{10}$: 603.1721, Found: 603.1725.

***D*-BQGA:** *D*-BQGA was synthesized as the above-mentioned procedures of *L*-BQGA except D-glutamic diethyl ester hydrochloride was used.

^{1}H NMR (400 MHz, DMSO-d_6, 298 K), see **Figure S14:** δ = 13.50-11.69 (m, 2H), 9.23 (s, 2H), 8.81 (s, 2H), 8.28 (t, J = 7.4 Hz, 4H), 7.91 (t, J = 7.6 Hz, 2H), 7.75 (t, J = 7.8 Hz, 2H), 4.62-4.51 (m, 2H), 2.44 (d, J = 7.6 Hz, 4H), 2.14 (d, J = 7.7 Hz, 2H), 1.98 (m, 2H).

^{13}C NMR (100 MHz, DMSO-d_6, 298 K), see **Figure S15:** δ = 174.16, 173.52 167.55, 154.75, 147.97, 144.08, 131.14, 130.16, 128.66, 125.97, 125.08, 116.05, 52.42, 30.83, 26.36.

HR-MALDI-TOF-MS, see **Figure S16:** m/z calcd. for $[M+H]^+$, $C_{30}H_{27}N_4O_{10}$: 603.1721, Found: 603.1718.

2. Supplementary figures.

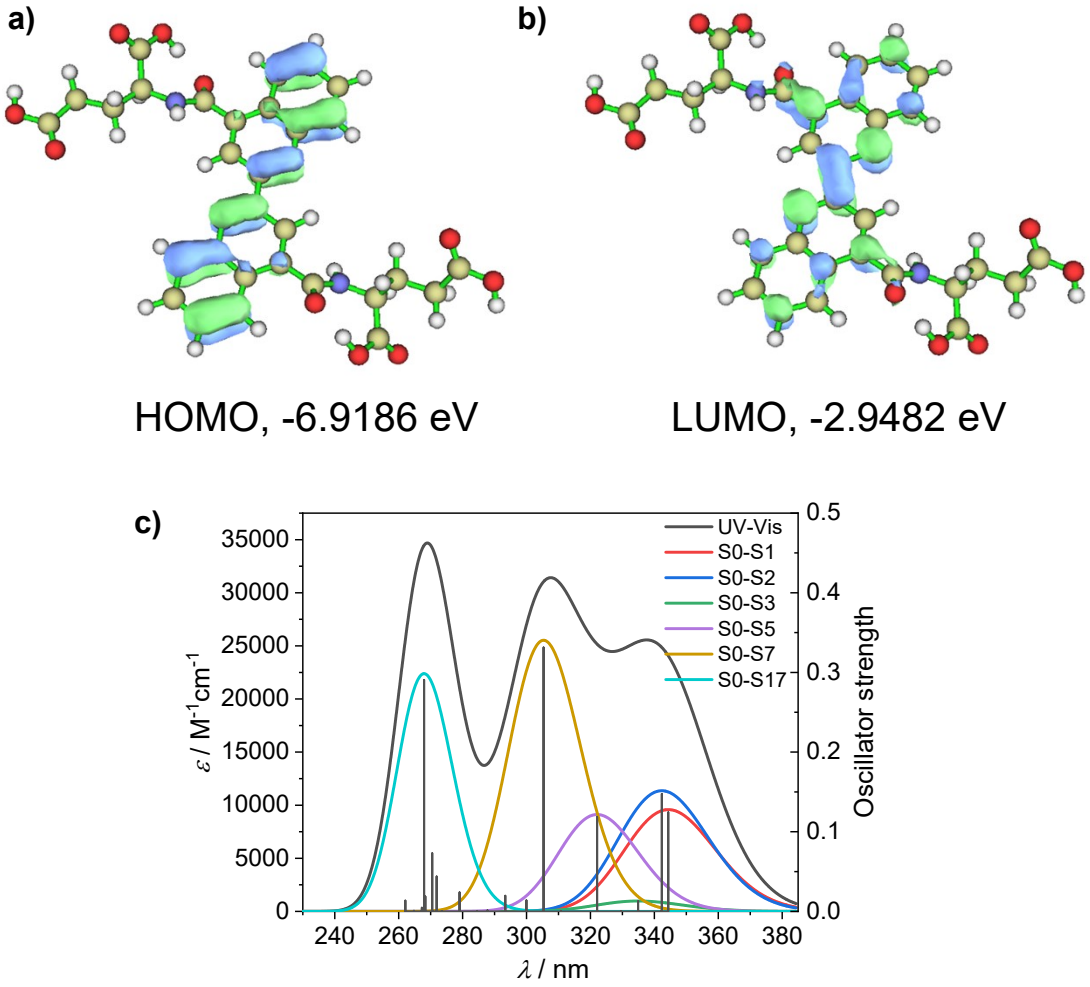

Figure S1. a) and b) Frontier molecular orbitals of BQGA calculated by DFT at B3LYP/6-311G(d) level.[1] The distributions of hole and electron is represented by the blue and green colors of the electron cloud. The carbon, oxygen, nitrogen, and hydrogen atoms of BQGA are represented by cyan orange, red, blue and gray balls, respectively.[2] c) Calculated UV-vis spectrum of BQGA (black line) and contributions of S0-S1 transition (red line), S0-S4 transition (blue line) and S0-S9 transition (green line). TD-DFT at B3LYP/6-311G(d) level. The black vertical lines represent oscillator strength of different electric transitions.

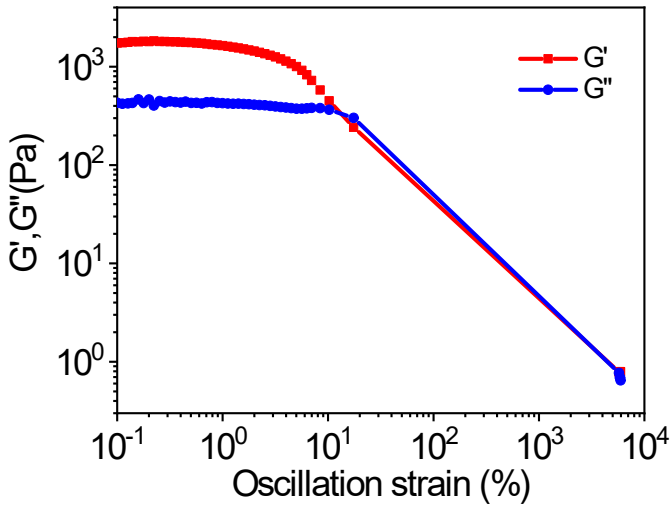

Figure S2. The change of storage modulus (G') and loss modulus (G'') of BQGA hydrogel along with oscillation strain.

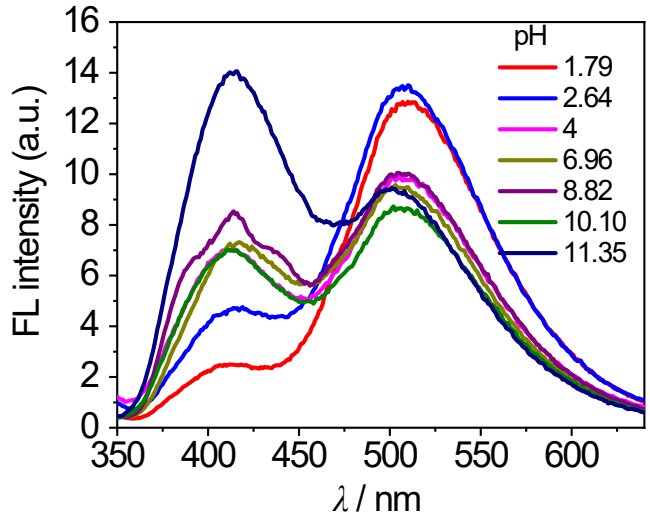

Figure S3. FL spectra of BQGA^{gel} with different pH values which are regulated by adding HCl and NaOH.

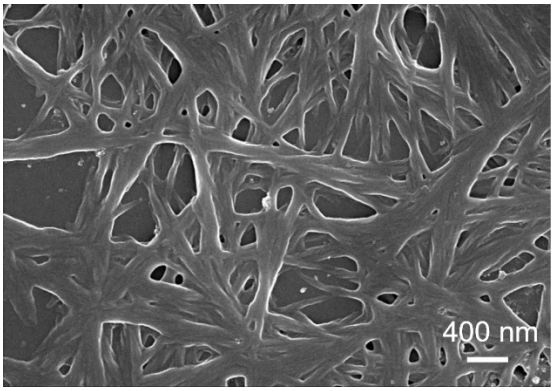

Figure S4. The SEM image of xerogel of D-BQGA. [BQGA] = 5 mM in H_2O.

Figure S5. Sunlight irradiation of $BQGA^{gel}$ in outdoor conditions. Photographs of $BQGA^{gel}$ before (left) and after (right) sunlight irradiation for 1 minute.

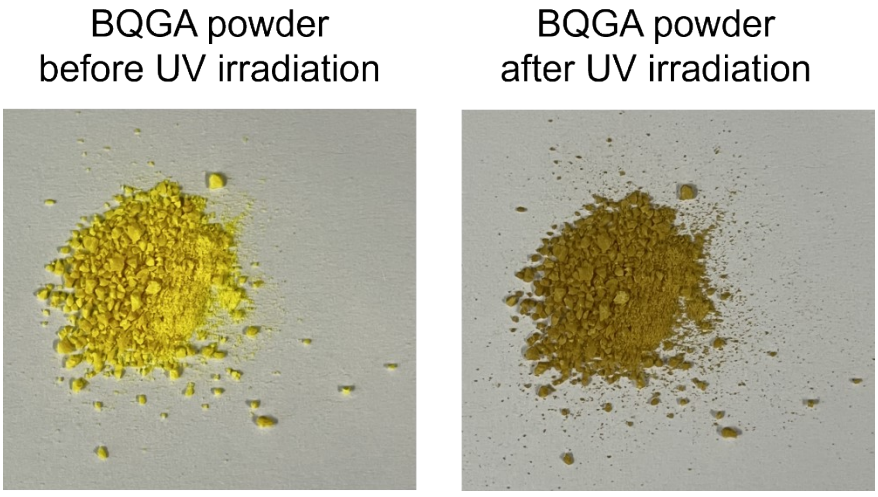

Figure S6. Photographs of BQGA powder before (left) and after (right) UV irradiation for 1 minute.

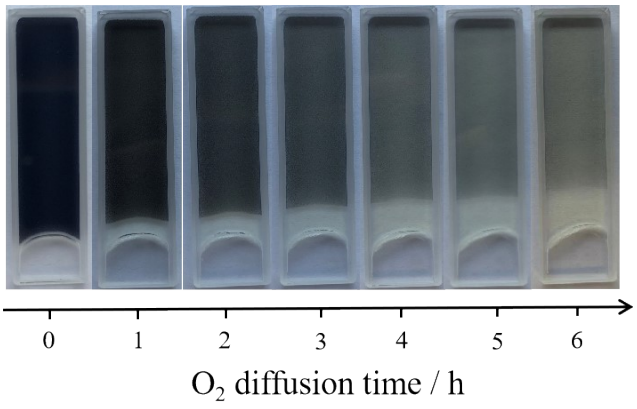

Figure S7. Oxygen diffusion experiment of BQGA radical hydrogel in ambient environment. The gel samples in an open cuvette were firstly exposed to ultraviolet light for 5 minutes. The cuvette sample was then placed in ambient environment.

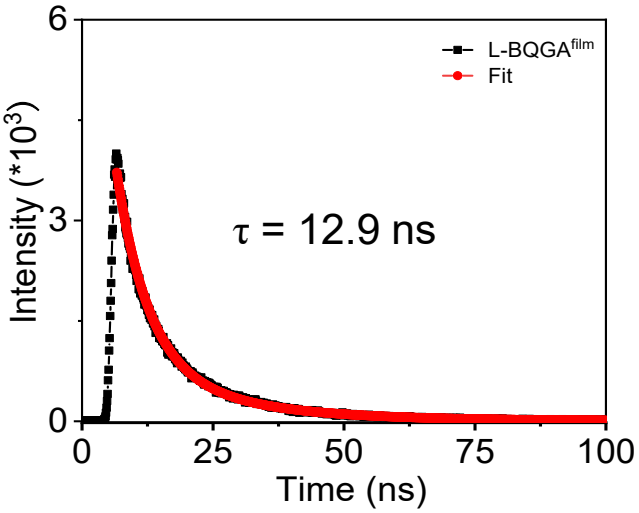

Figure S8. Emission decay curves of *L*-BQGA^{film}. Excitation wavelength is 310 nm. Emission wavelength decay at 500 nm. τ represents average fluorescence lifetime. [BQGA] = 5 mM.

Table S1. Crystal data and structure refinement for *L*-BQGA.

	***L*-BQGA**
Empirical formula	$C_{36}H_{44}N_4O_{13}S_3$
Formula weight	836.93
Temperature/K	169.99(14)
Crystal system	monoclinic
Space group	$P2_1$
a/Å	17.0638(3)
b/Å	4.99240(10)
c/Å	23.7104(4)
α/°	90
β/°	101.092(2)
γ/°	90
Volume/Å^3	1982.14(6)
Z	2
ρ_{calc}g/cm^3	1.402
μ/mm^{-1}	2.302
F(000)	880.0
Crystal size/mm^3	0.2 × 0.02 × 0.01
Radiation	Cu Kα (λ = 1.54184)
2Θ range for data collection/°	3.798 to 154.82
Index ranges	-18 ≤ h ≤ 21, -6 ≤ k ≤ 6, -29 ≤ l ≤ 29
Reflections collected	37145
Independent reflections	8038 [Rint = 0.0864, Rsigma = 0.0418]
Data/restraints/parameters	8038/44/591
Goodness-of-fit on F^2	1.056
Final R indexes [I>=2σ (I)]	R1 = 0.0740, wR2 = 0.1921
Final R indexes [all data]	R1 = 0.0792, wR2 = 0.1962
Largest diff. peak/hole / e Å^{-3}	0.44/-0.79
Flack parameter	0.051(11)

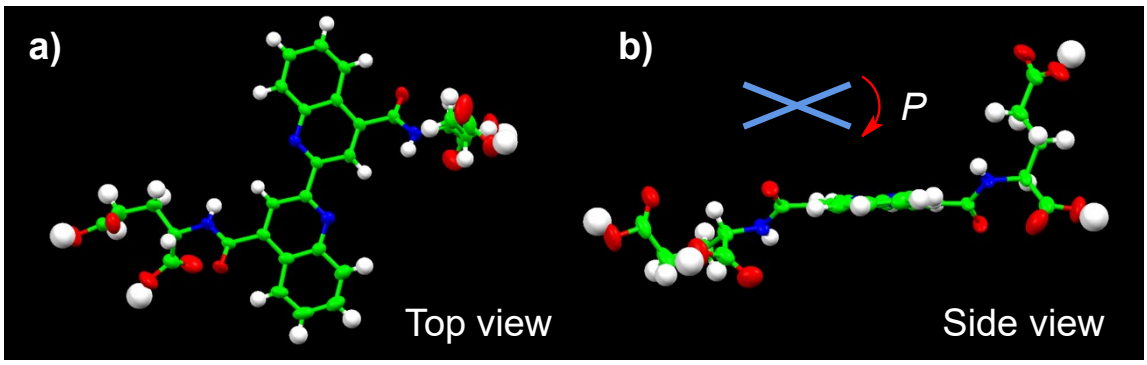

Figure S9. Single crystal structures of *L*-BQGA, a) Top View, b) Side View. The inserted image in b) indicates the relative rotation of the two quinoline chromophores from side view.

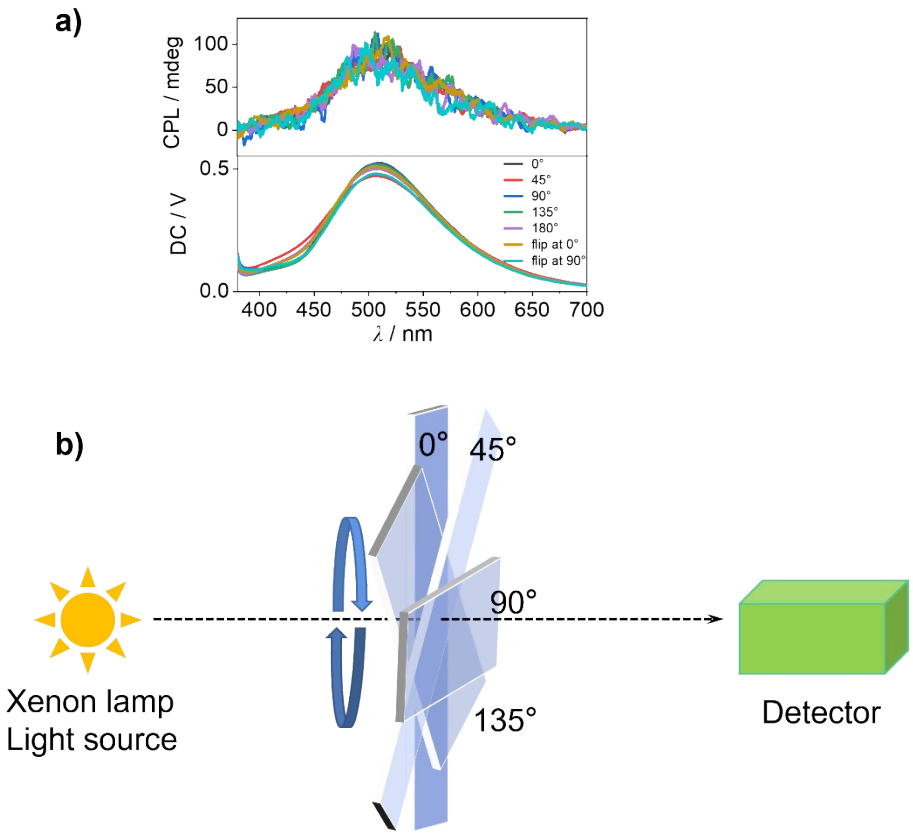

Figure S10. a) CPL spectra and b) Schematic illustration of measuring CPL signals by rotating and flipping the BQGA thin film.

3. Additional spectra.

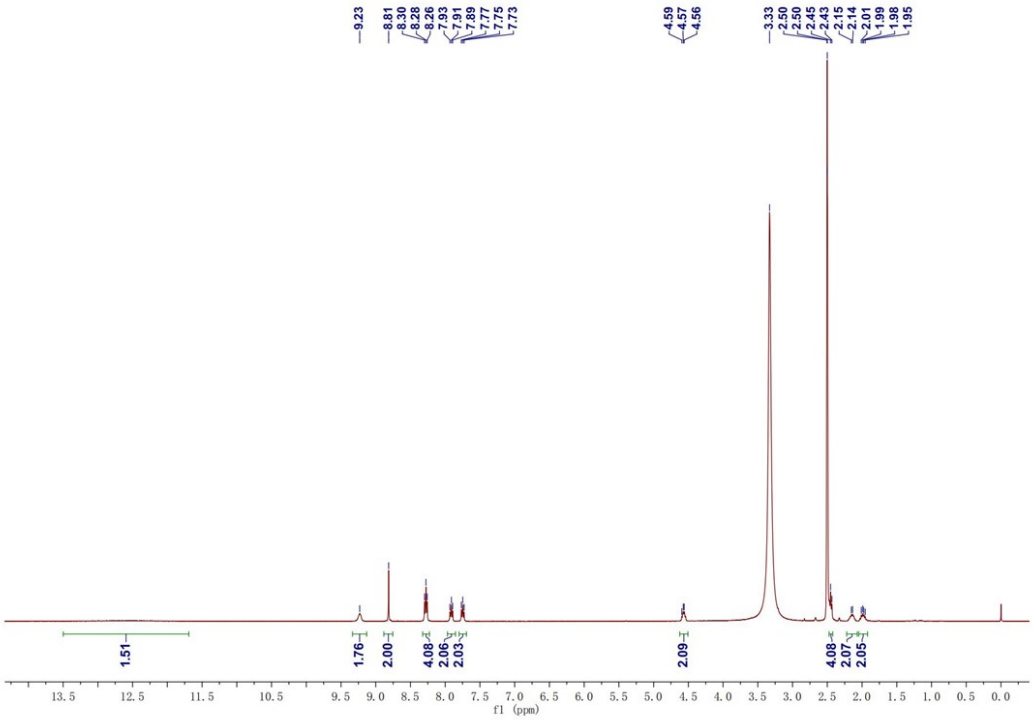

Figure S11. ^{1}H-NMR spectrum of *L*-BQGA (400MHz, DMSO-d_6, 298 K).

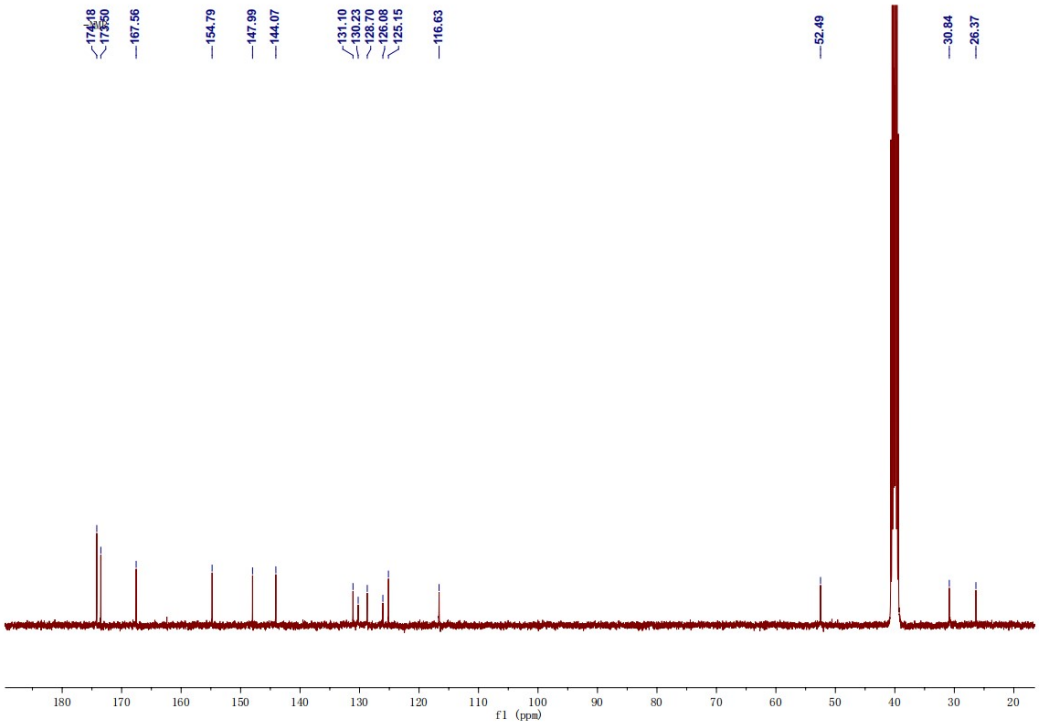

Figure S12. ^{13}C-NMR spectrum of *L*-BQGA (100 MHz, DMSO-d_6, 298 K).

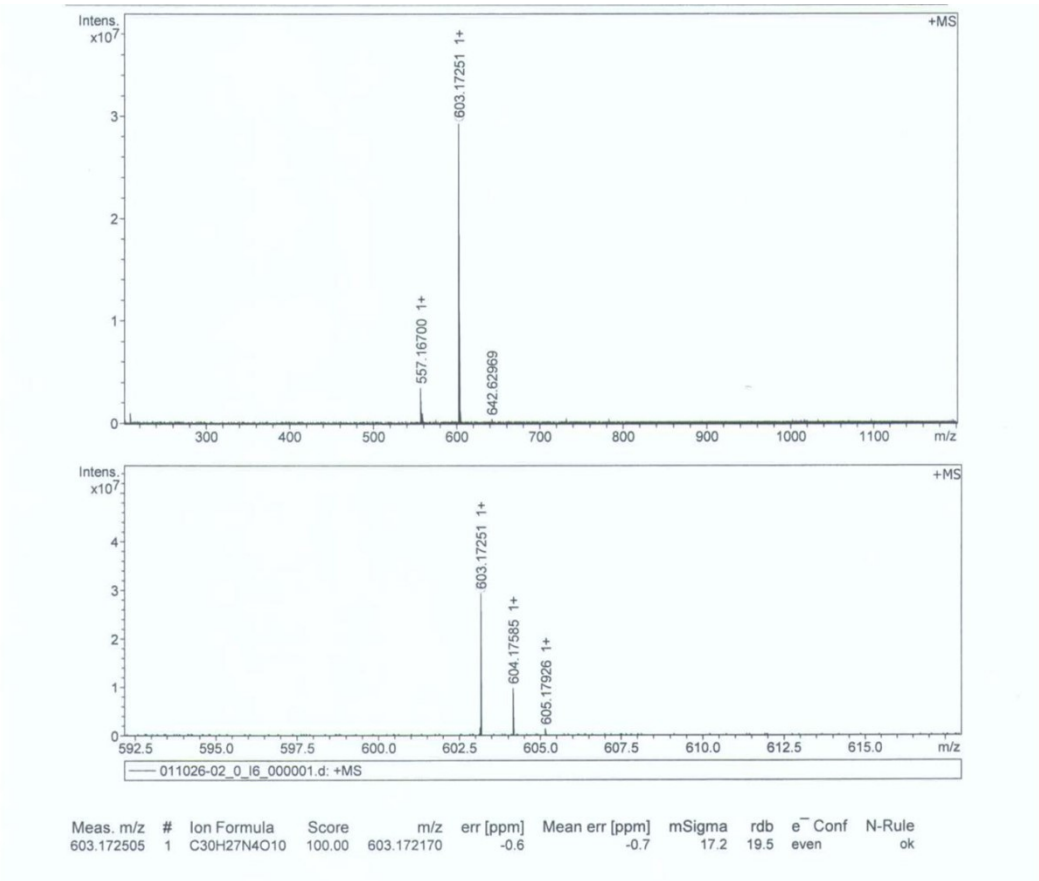

Figure S13. The HR-MALDI-FTICR-MS spectrum of *L*-BQGA.

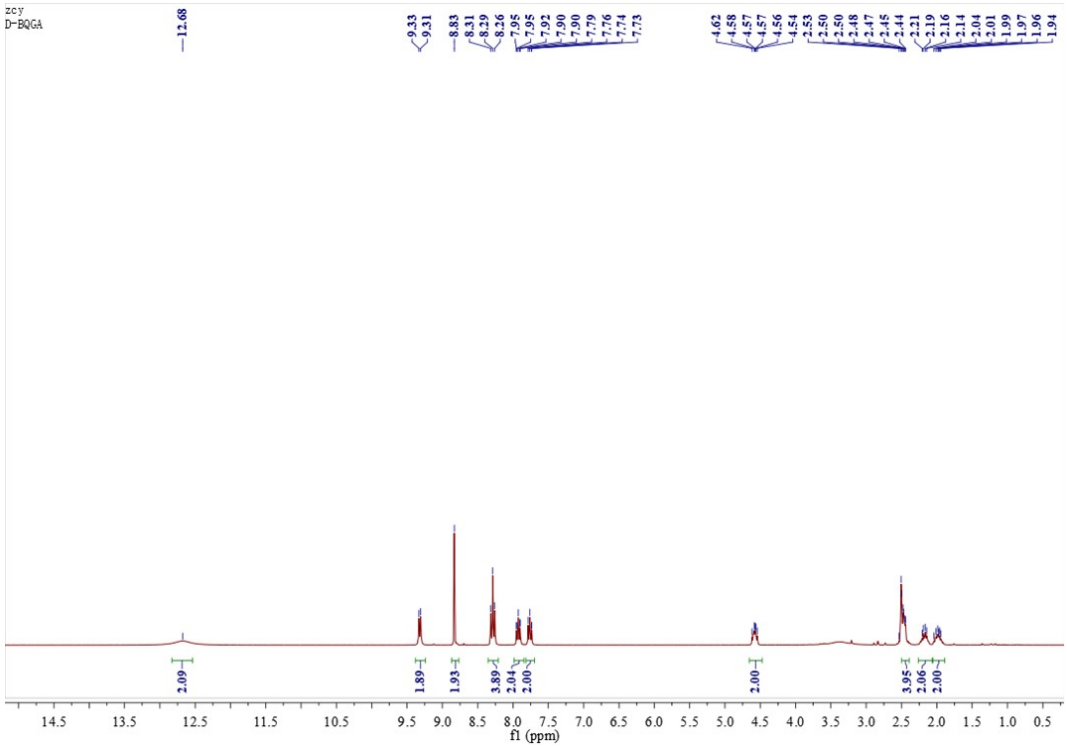

Figure S14. ^{1}H-NMR spectrum of *D*-BQGA (400MHz, DMSO-d_6, 298 K).

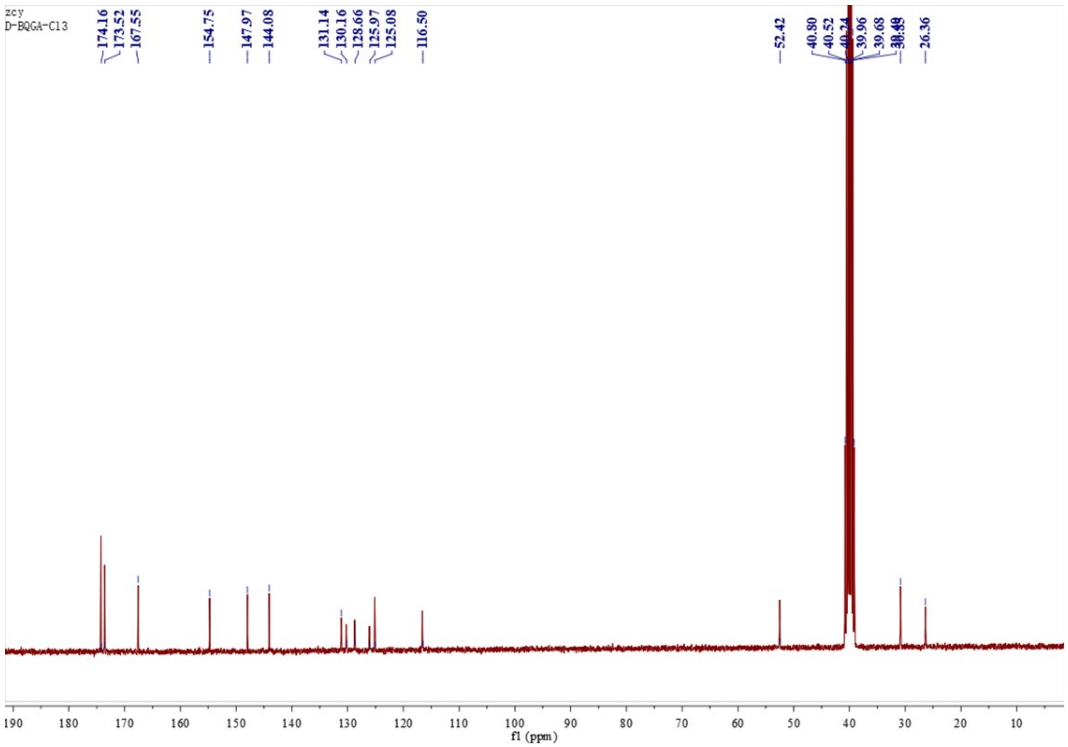

Figure S15. ^{13}C-NMR spectrum of *D*-BQGA (100 MHz, DMSO-d_6, 298 K).

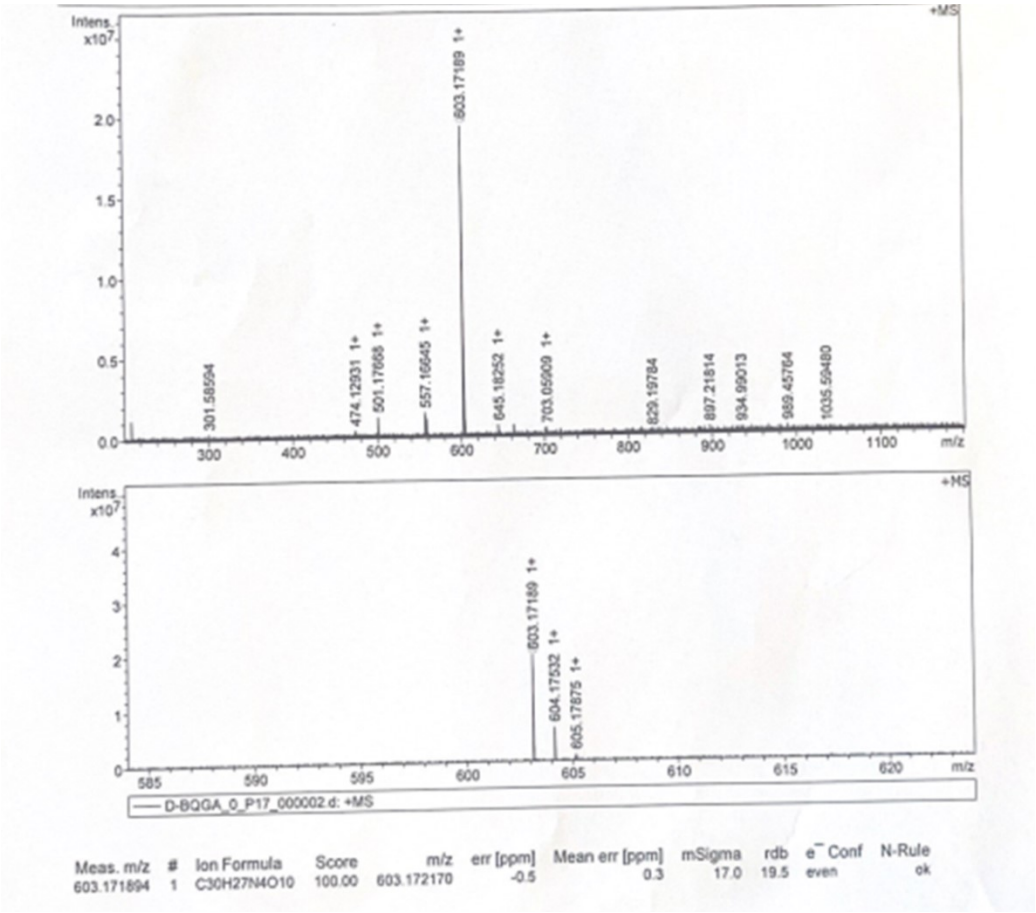

Figure S16. The HR-MALDI-FTICR-MS spectrum of *D*-BQGA.

4. Experimental methods

Materials. All chemicals and solvents were used without further purification. 2,2'-biquinoline-4,4-dicarboxylic acid was purchased from J&K. *L*- and *D*- glutamic diethyl ester hydrochlorides were purchased from TCI. 1-hydroxybenzotriazole (HOBt, >98.0%), 1-(3-dimethylaminopropyl)-3-ethylcarbodiimide hydrochloride (EDC•HCl, >98.0%) and triethylamine were purchased from J&K. LiOH (AR, Beijing Chemical Works), Na_2SO_4 (AR, Beijing Chemical Works), $NaHCO_3$ (AR, Beijing Chemical Works), Milli-Q water (18.2 MΩ·cm), N,N'-Dimethylformamide (DMF, AR, Concord Technology (Tianjin) Co., Ltd), Methanol (MeOH, AR, Concord Technology (Tianjin) Co., Ltd), The synthetic procedures of L-BQGA and D-BQGA were listed in Scheme S1, supplementary information. The products were purified by column chromatography and characterized by ^{1}H NMR, ^{13}C NMR and MALDI-FTICR-MS.

BQGA^{gel} sample preparation. 3.00 mg *L*-BQGA or *D*-BQGA sample was dispersed into 1 mL H_2O in a 4 mL sample vial. The mixture was heated until the solid was entirely dissolved and a yellow transparent solution was obtained. After natural cooling to room temperature, a yellow clear gel was formed and used for other measurements.

BQGA^{film} sample preparation. 3.00 mg *L*-BQGA or *D*-BQGA sample was dissolved into 1 mL methanol solvents in a 4 mL sample vial. Drop-casting of 200 μL solution with a pipette onto a piece of quartz (1.5 cm × 4.5 cm) at room temperature obtained a BQGA film.

Ultraviolet-visible absorption spectra. The samples were recorded on a U-3900 (Hitachi) UV-vis spectrophotometer.

Fluorescence spectra. The fluorescence spectra were recorded on a F-4500 fluorescence spectrophotometer (Hitachi). The testing voltage was 400 V, the width

of the excitation and emission slits were 5 nm, the scanning speed was 1200 nm/min. Fluorescence quantum yields were measured on a FluoroMax+ (HORIBA) instrument by using an integrating sphere. The fluorescence decay curves were recorded on a FLS 980 spectroscopy (Edinburgh Instruments). The wavelength of the excitation laser was 310 nm.

Circular dichroism (CD) spectra. CD spectrometer J-1500 (JASCO) at a scanning rate of 500 nm min^{-1}.

Circularly polarized luminescence (CPL) spectra. CPL spectra were measured with JASCO CPL-300 spectrophotometer in the range of 400 ~ 700 nm with a scanning rate of 500 nm/min. CPL spectra were converted to g_{lum} spectra using SpectraManager (JASCO) software.

NMR spectra. ^{1}H NMR, ^{13}C NMR spectra were recorded on a Bruker ADVANCE III 400 (^{1}H: 400 MHz ^{13}C: 100 MHz) spectrometer in DMSO-d_6 at 298 K.

Mass spectra. Mass spectrum data were obtained by using a BIFLEIII matrix-assisted laser desorption/ionization time of fight mass spectrometry (MALDI-FTICR-MS) instrument, the sample was dissolved in MeOH and volatilized on the substrate for testing.

Scanning electron microscopy (SEM). Solution aggregates or solid powders were casted on a silicon wafer. After dried under vacuum, the sample was coated with a thin layer of Au and Pt to increase the contrast, which was then recorded on a Hitachi S-4800 FE-SEM instrument with an accelerating voltage of 10 kV and an operating current of 10 μA.

Fourier transform infrared (FT-IR). FT-IR spectra were recorded on a Bruker TENSOR-27 FT-IR spectrometer. The KBr pellets of the vacuum-dried samples were submitted for FT-IR spectra measurement. The test wavenumber ranges from 400 to 4000 cm^{-1}.

Single crystal X-ray diffraction. The data were collected on an XtaLAB Synergy-R diffractometer. The structures were solved by direction methods and refined by a full matrix least squares technique based on F2 using SHELXL 97 program (Sheldrick, 1997). The crystal packing was obtained using the software Mercury 1.4.1. *L*-BQGA crystals suitable for X-ray diffraction were obtained by slow diffusion of ethyl acetate in DMSO solution.

X-ray diffraction (XRD) measurements. PXRD analysis was performed on a Rigaku D/Max-2500 X-ray diffractometer with Cu/Kα radiation (λ = 1.5406 Å), which was operated at a voltage of 40 kV and a current of 200 mA. Samples were prepared on single crystal silicon wafer and vacuum dried for PXRD testing. The scanning range was from 1~30°

Density functional theory (DFT) computation. DFT and time-dependent DFT calculations were performed by Gaussian 09 program at B3LYP 6-311G(d) level.

5. Supporting references

1. M. J. Frisch, G. W. Trucks, H. B. Schlegel, G. E. Scuseria, M. A. Robb, J. R. Cheeseman, G. Scalmani, V. Barone, B. Mennucci, G. A. Petersson, H. Nakatsuji, M. Caricato, X. Li, H. P. Hratchian, A. F. Izmaylov, J. Bloino, G. Zheng, J. L. Sonnenberg, M. Hada, M. Ehara, K. Toyota, R. Fukuda, J. Hasegawa, M. Ishida, T. Nakajima, Y. Honda, O. Kitao, H. Nakai, T. Vreven, J. A. Montgomery, Jr., J. E. Peralta, F. Ogliaro, M. Bearpark, J. J. Heyd, E. Brothers, K. N. Kudin, V. N. Staroverov, T. Keith, R. Kobayashi, J. Normand, K. Raghavachari, A. Rendell, J. C. Burant, S. S. Iyengar, J. Tomasi, M. Cossi, N. Rega, J. M. Millam, M. Klene, J. E. Knox, J. B. Cross, V. Bakken, C. Adamo, J. Jaramillo, R. Gomperts, R. E. Stratmann, O. Yazyev, A. J. Austin, R. Cammi, C. Pomelli, J. W. Ochterski, R. L. Martin, K. Morokuma, V. G. Zakrzewski, G. A. Voth, P. Salvador, J. J. Dannenberg, S. Dapprich, A. D. Daniels, O. Farkas, J. B. Foresman, J. V. Ortiz, J. Cioslowski, and D. J. Fox, Gaussian 09, Revision D.01, Gaussian, Inc., Wallingford CT, 2013.

2. T. Lu and F. Chen, *J. Comput. Chem*. 2012, **33**, 580-592.